ACS APPLIED MATERIALS & INTERFACES

Research Article

www.acsami.org

Al_2O_3 on Black Phosphorus by Atomic Layer Deposition: An *in Situ* Interface Study

Hui Zhu,[†] Stephen McDonnell,[†] Xiaoye Qin,[†] Angelica Azcatl,[†] Lanxia Cheng,[†] Rafik Addou,[†] Jiyoung Kim,[†] Peide D. Ye,[‡] and Robert M. Wallace*[,†]

[†]Department of Materials Science and Engineering, University of Texas at Dallas, Richardson, Texas 75080, United States

[‡]School of Electrical and Computer Engineering and Birck Nanotechnology Center, Purdue University, West Lafayette, Indiana 47907, United States

Supporting Information

ABSTRACT: *In situ* "half cycle" atomic layer deposition (ALD) of Al_2O_3 was carried out on black phosphorus ("black-P") surfaces with modified phosphorus oxide concentrations. X-ray photoelectron spectroscopy is employed to investigate the interfacial chemistry and the nucleation of the Al_2O_3 on black-P surfaces. This work suggests that exposing a sample that is initially free of phosphorus oxide to the ALD precursors does not result in detectable oxidation. However, when the phosphorus oxide is formed on the surface prior to deposition, the black-P can react with both the surface adventitious oxygen contamination and the H_2O precursor at a deposition temperature of 200 °C. As a result, the concentration of the phosphorus oxide increases after both annealing and the atomic layer deposition process. The nucleation rate of Al_2O_3 on black-P is correlated with the amount of oxygen on samples prior to the deposition. The growth of Al_2O_3 follows a "substrate inhibited growth" behavior where an incubation period is required. *Ex situ* atomic force microscopy is also used to investigate the deposited Al_2O_3 morphologies on black-P where the Al_2O_3 tends to form islands on the exfoliated black-P samples. Therefore, surface functionalization may be needed to get a conformal coverage of Al_2O_3 on the phosphorus oxide free samples.

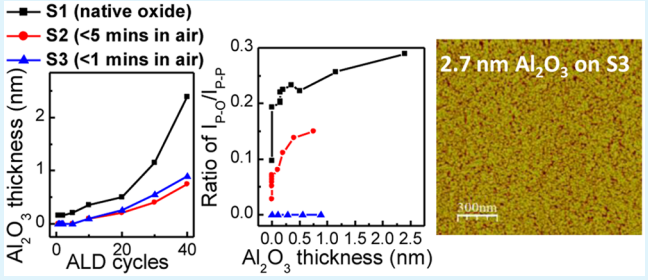

KEYWORDS: *black phosphorus, surface oxidation, atomic layer deposition, aluminum oxide, water, X-ray photoelectron spectroscopy*

1. INTRODUCTION

Black phosphorus ("black-P") is an anisotropic lamellar semiconductor considered to be an appealing two-dimensional (2D) material because of its novel properties and potential application in few-layer transistor structures.[1−7] Bulk black-P has a direct bandgap of about 0.3 eV,[2,8,9] and an impressive hole mobility of up to 10^4 $cm^2/(V·s)$ at low temperatures (50−100 K).[10,11] Few-layer black-P field effect transistors possess high current on/off ratios (up to 10^4) and high carrier mobilities up to 1000 $cm^2/(V·s)$ at room temperature.[1,2] Consequently, black-P is a promising candidate for nanoelectronic and optoelectronic device applications.[12] However, a clear challenge in the implementation of black-P is the strong hydrophilic[13,14] and oxidation[9] reactions during device processing and thereafter. Thus, efficient isolation/passivation layers are necessary for black-P to preserve its electronic properties. To date, many efforts on passivation have been reported. For example, recent reports show that the high field-effect mobility (~1350−4000 $cm^2/(V·s)$) of a hexagonal boron nitride (h-BN) isolated BN/black-P/BN heterostructure[15−17] is stable in an atmospheric ambient for more than 1 week. Al_2O_3[2,3,18] or HfO_2[19] dielectric layers deposited by atomic layer deposition (ALD) are also used as passivation layers in recent black-P transistors. Luo et al.[3] and Wood et al.[13] mentioned that the Al_2O_3 passivated few-layer black-P metal oxide semiconductor field-effect transistors (MOSFET) can be stable in air for more than 100 h. However, there are still many unsolved problems for high-k/black-P heterostructures such as lower field mobilities (40−100 $cm^2/(V·s)$) with respect to BN/black-P/BN and trapped charge issues.[2,3,13] It is still unclear whether surface oxidation by ambient conditions degenerates the electronic properties of ALD Al_2O_3/black-P. Toward this end, three different samples oxidized by ambient air were investigated to understand the interfacial interaction, chemistry, and nucleation of atomic layer deposited Al_2O_3 on black-P using a combination of *in situ* monochromatic X-ray photoelectron spectroscopy (XPS) and *ex situ* atomic force microscopy (AFM).

2. EXPERIMENTAL SECTION

Three black-P samples (thickness ~1 mm), synthesized and purchased from Smart Elements, were used in this study. One is examined "as received" with a native oxide ("S1") present on the surface, and another two ("S2" and "S3") were cleaned by mechanical exfoliation

Received: April 13, 2015
Accepted: May 28, 2015

DOI: 10.1021/acsami.5b03192
ACS Appl. Mater. Interfaces XXXX, XXX, XXX−XXX

with Scotch Magic tape, which removes the outer layers of the crystal before loading the samples in ultrahigh vacuum (UHV). The UHV system used in this work was described in detail elsewhere[20] and connects a surface analysis chamber and a Picosun 200R ALD chamber (base pressure ~4 mbar) through a UHV (~10^{-10} mbar) transfer tube, preventing spurious surface contamination during the experiment. To control surface oxidation, the S2 sample was oxidized by ambient air exposure for 5 min, whereas the S3 sample was loaded into the UHV chamber immediately after exfoliation (less than 2 min ambient exposure). In this experiment, ALD of Al_2O_3 was carried out with successive cycles of trimethylaluminum (TMA) and H_2O precursors, with an argon (Ar) carrier gas (99.9997%, Airgas) at a flow rate of 200 sccm, 0.1 s pulse + 4 s Ar purge time for TMA, 0.1 s pulse + 6 s Ar purge time for H_2O at a substrate temperature of 200 °C. To monitor the Al_2O_3 growth on black phosphorus, the XPS scans were taken as follows: (i) on the initial surfaces, (ii) after exposing samples to the ALD vacuum ambient at 200 °C for 1 h, (iii) after each successive half cycle[21] of TMA and H_2O up to two full cycles, as well as after (iv) 5, 10, 20, 30, and 40 full cycles (TMA + H_2O). Additional XPS scans were performed on the S3 sample after 60 and 80 full cycles.

XPS spectra were taken of the P 2*p*, Al 2*p*, Sn 3*d*, I 3*d*, C 1*s* and O 1*s*, core level regions using a monochromatic Al Kα X-ray source ($h\nu$ = 1486.7 eV) with a takeoff angle of 45° from the substrate normal and a pass energy of 15 eV. The deconvolution of XPS was carried out with AAnalyzer software.[22] The AFM images of the samples after 40 cycles of Al_2O_3 were recorded on three samples using an *ex situ* Veeco (Bruker) multimode system in noncontact tapping mode. To compare the Al_2O_3 growth on the S1 and S3 samples, AFM images were also obtained on the S3 sample after 80 cycles of Al_2O_3, which has a comparable Al_2O_3 thickness to that of the S1 sample. The AFM images were analyzed using WSxM software.

3. RESULTS AND DISCUSSION

Figure 1a compares the deconvolution of P 2*p* core level XPS spectra from the S1, S2, and S3 samples during the first stages of the ALD process. On the initial sample surfaces, the concentration of the oxidized phosphorus species (labeled as PO_x, e.g., P_2O_3)[23] at 134.2 eV clearly increases with ambient air exposure time: S1 shows the highest oxide concentration, whereas sample S2 is slightly oxidized and the oxidation is below the XPS detection limit (~0.1 at.%) for sample S3. In Figure 1b, integrated intensity ratio of the total phosphorus oxide ($I_{P\text{-}O}$) feature to the integrated intensity of the bulk black-P feature ($I_{P\text{-}P}$) is shown. The $I_{P\text{-}O}/I_{P\text{-}P}$ ratios on the initial S1 and S2 samples are estimated to be 0.1 and 0.03, respectively. The phosphorus oxide thicknesses were estimated, using XPS peak attenuation (see the Supporting Information) for samples S1 and S2, to be ~0.27 and ~0.08 nm, respectively.

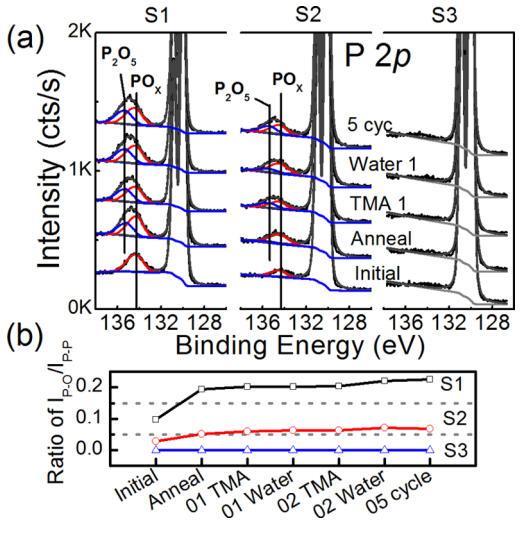

Figure 1. (a) XPS spectra are showing the evolution of P 2*p* core level from the S1, S2, and S3 samples during the half cycle ALD process. Phosphorus oxide is below the limit of detection on the S3 sample. (b) Integrated intensity ratio of the total phosphorus oxide to that of the bulk black-P peak ($I_{P\text{-}O}/I_{P\text{-}P}$), up to the initial 5 ALD cycles for the S1, S2, and S3 samples, respectively.

To differentiate clearly between thermal effects and surface reactions with ALD precursors, the three samples were exposed to the ALD reactor environment at 200 °C for 1 h under Ar flow (P ~4 mbar), and were subsequently analyzed by XPS without any ALD precursor exposure. After this process, a saturated phosphorus oxide chemical state (P_2O_5)[24−26] is clearly detected at 135.1 ± 0.05 eV on the S1 sample. This feature is also observed with a lower intensity on the S2 sample. The intensity ratio $I_{P\text{-}O}/I_{P\text{-}P}$ (seen in Figure 1b) after annealing increases to 0.2 and 0.05 on the S1 and S2 samples, respectively, while remaining below the XPS detection limit on the S3 sample. The estimated phosphorus oxide thicknesses after annealing are ~0.33 and ~0.13 nm for samples S1 and S2, respectively. In addition, the original PO_x peak (at 134.2 eV) does not decrease after annealing, suggesting that the formation of P_2O_5 originates from the adsorption of oxygen, not only the conversion from PO_x to P_2O_5 with temperature. Oxygen sources are likely the surface adventitious contamination such as O−C(H) species that are detectable on every sample (shown in the Supporting Information Figures S1 and S2). A similar phenomenon is also found in our previous ALD half cycle study of AlGaN, where the surface oxygen contamination results in the increase of Ga/Al−O concentration during the initial annealing prior to ALD.[27−29] Recent density functional theory (DFT) calculations suggest that the most favorable sites for oxygen on black-P depends on the amount of oxygen being adsorbed.[30] Considering the reaction of an oxygen atom[24,30] or an O_2 molecule[30] with an ideal, defect free black-P surface, the direct adsorption of oxygen on top of a single P atom, with the underlying black-P structure remaining unchanged, is relatively more favorable than bridging between two P atoms for low oxygen concentrations, such as <1 oxygen per unit cell.[24,30] For a higher oxygen concentration (>2 oxygen atoms per unit cell), both direct adsorption on top of a single P atom and also bridge bonding between two P atoms are energetically favorable and result in the formation of planar or tubular phosphorus oxides such as P_2O_3 or P_2O_5.[30] It should be noted that the lattice constants of some phosphorus oxides, such as tubular-P_2O_5, can be 1.9 times larger than that of black-P, leading to obvious black-P lattice deformation through bond scission and O insertion.[30] Therefore, in samples S1 and S2, the higher concentration of phosphorus oxides with respect to S3 can be correlated with a higher probability of black-P lattice deformation. It is not surprising then that the samples with the highest concentration of initial oxides are found to be the most reactive when exposed to identical oxidizing environments.

It is interesting to note that during the following half cycle ALD process, there is no detectable phosphorus oxides within the range of 133−136 eV on sample S3, indicating that S3 is essentially phosphorus oxide free. To confirm the reproducibility, a second phosphorus oxide free sample was prepared and analyzed by XPS after atomic layer deposition, the results of which are shown in Figure S3 of the Supporting Information. These results are consistent and indicate that the TMA or water

DOI: 10.1021/acsami.5b03192
ACS Appl. Mater. Interfaces XXXX, XXX, XXX−XXX

precursor does not react with the black-P surface under vacuum. The main O 1*s* peak (~531.5−533 eV) detected from the initial S3 sample (see Figure S1 of the Supporting Information) corresponds to the physisorbed O−C(H) species. This phenomenon is consistent with recent DFT calculations, which show that water adsorption on a bilayer black-P can occur without phosphorus oxidation.[14] Favron et al.[9] also show that after black-P is exposed to water under vacuum, no degradation of black-P is detected. Based on our experimental findings, the increased oxides after annealing and the following half cycle ALD process observed on S1 and S2 samples, are mainly related to the presence of the initial phosphorus oxide itself.

The growth of Al_2O_3 on the three samples is quite different, as can be seen in Figure 2a, which shows the thickness of Al_2O_3

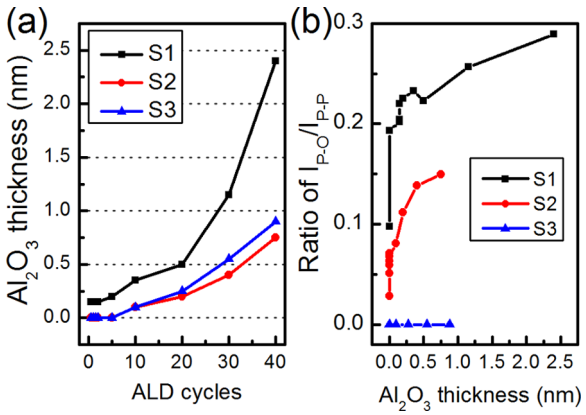

Figure 2. (a) Al_2O_3 thickness during the ALD process for the S1, S2, and S3 samples. (b) Ratio of $I_{P\text{-}O}/I_{P\text{-}P}$ as a function of Al_2O_3 thickness.

as a function of ALD cycles on all three substrates. The thickness is calculated from the attenuation of the P 2*p* peak (see the Supporting Information). Focusing first on samples S1 and S2, which both started with detectable phosphorus oxide concentrations, it is clear that the growth rate on S1 is significantly higher. This can be explained by the higher concentration of nucleation sites afforded by the increased defects and phosphorus oxide concentration. The relatively slow growth rate (<1 Å/cycle) at the initial stage indicates that ALD Al_2O_3 requires several cycles to nucleate on the black-P substrate and displays "substrate-inhibited growth".[27,28,31] Once a thickness of approximately 0.5 nm is reached the growth rate is seen to noticeably increase suggesting that the growth mechanism has changed. Considering that this thickness corresponds to one monolayer of Al_2O_3 within experimental error, the two growth regimes can be identified as ALD on black-P and (mainly subsequent) ALD on Al_2O_3. After 40 cycles, the Al_2O_3 thickness is ~2.47, 0.74, and 0.88 nm on the S1, S2, and S3 samples, respectively. As Figure 1(a) shows, after 30 cycles on the S1 sample, the growth rate increases to 1 Å/cycle, so the initial 30 cycles is the incubation period for the native oxidized sample; whereas for S2 and S3 samples, the Al_2O_3 growth rate within 40 cycles is still much lower than 1 Å/cycle. This behavior suggests that the incubation cycles for samples S2 and S3 are more than 40 cycles.

The slightly thicker Al_2O_3 on the S3 than that on the S2 sample deserves discussion because S3 had initially no detectable phosphorus oxide. As discussed earlier, the lack of phosphorus oxide does not necessarily mean an absence of oxygen and in fact a detailed analysis of the O 1*s* spectra (shown in Figure S1 of the Supporting Information), shows that the total concentration of oxygen on the surface is actually higher for S3 than for S2. This strongly suggests that surface adventitious contamination could also enhance the nucleation of Al_2O_3[32] and become the dominant mechanism in the case of low PO_x concentration.

Because the growth rates on these samples are different, a quantitative comparison of the rate of phosphorus oxidation as a function of ALD cycles (shown in Figure S4 of the Supporting Information) is not as meaningful as considering the reactions as a function of ALD thickness. Figure 2b shows the ratio of $I_{P\text{-}O}/I_{P\text{-}P}$ as a function of Al_2O_3 thickness. This ratio can be directly correlated to the concentration of thickness of phosphorus oxides. The ratio plateaus for samples S1 and S2 are very similar so that, once the deposited Al_2O_3 thickness is more than 1 monolayer (~0.5 nm), the oxidation rate of the black-P surface decreases due to the nonconformal coverage of Al_2O_3 films, which reduces the available interaction area of the black-P substrate with the water precursor. It is noted that the shakeup loss feature of Al 2*s*, which overlaps with P 2*p*, discussed in the Supporting Information (Figure S5), has a negligible effect on accurately determining the intensity of the P 2*p* peak.

Figure 3 shows the Al 2*p* core level XPS spectra from samples S1, S2, and S3 during the ALD process. The trend in

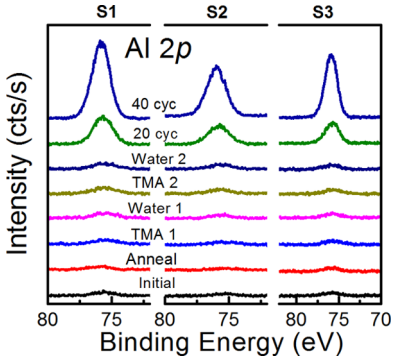

Figure 3. Al 2*p* core level spectra from the S1, S2, and S3 samples during the ALD process.

the Al 2*p* core-level intensities qualitatively matches the thicknesses determined by the P 2*p* attenuation, however, they are quantitatively different. If the thickness of Al_2O_3 on S2 is assumed to be 2.5 nm, as calculated by the P 2*p* attenuation, then the intensity ratio of the Al 2*p* core-levels for S1 and S2 (1.5 for S1:S2) would suggest that the thickness of Al_2O_3 on S2 is 1.2 nm, which does not agree with the value of 0.7 nm that was calculated by the P 2*p* peak attenuation. This suggests that for S2 and S3, there is more Al_2O_3 on the surface than is expected from only considering the attenuation of the P 2*p* feature. This can be explained after studying the topography of the samples.

Figure 4a−c shows the AFM images after 40 cycles of Al_2O_3 deposited on the S1, S2, and S3 samples, respectively, with representative line profiles. The root-mean-squared (RMS) roughness on the S1, S2, and S3 sample is ~0.22, ~0.34, and ~0.38 nm, respectively, and the vertical depth variation of the corresponding line profile is ~0.5, ~1 nm, and ~1 nm, respectively. This result immediately explains the conflicting thickness calculations using the Al 2*p* and P 2*p* core-levels

DOI: 10.1021/acsami.5b03192
ACS Appl. Mater. Interfaces XXXX, XXX, XXX−XXX

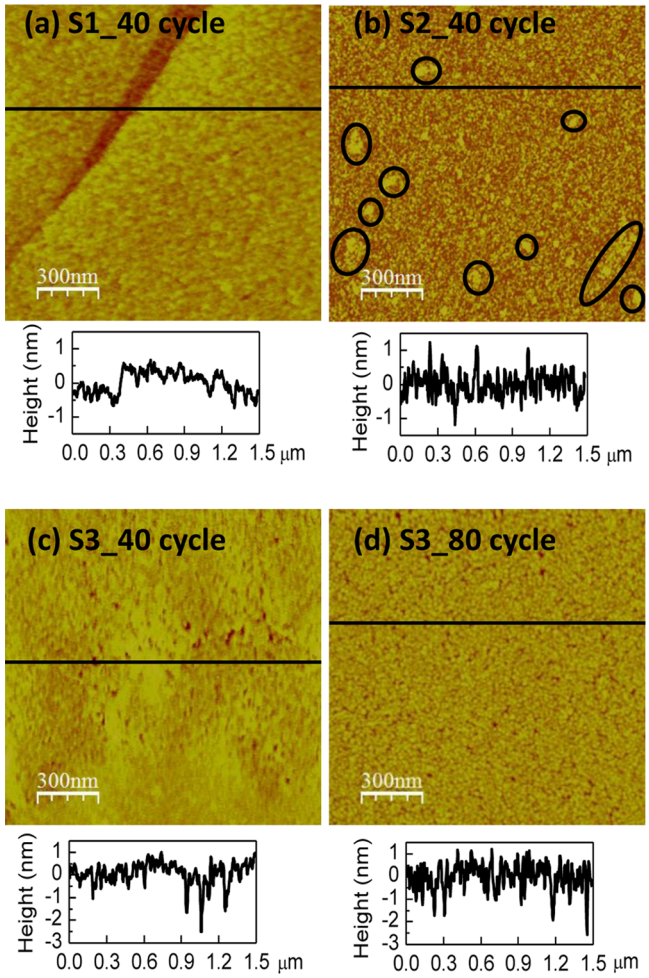

Figure 4. AFM images after 40 cycles of Al_2O_3 deposition on the (a) S1, (b) S2, and (c) S3 samples. (d) AFM image after 80 cycles of Al_2O_3 on S3. Line profiles are performed along the black lines shown on the AFM images. Step edge on the S1 sample is ~2 layers based on the black-P bulk crystal.

because the island growth observed can result in considerable deposition of Al_2O_3 without fully covering (and thereby more aggressively attenuating) the underlying substrate.

In addition, the surface morphology of Al_2O_3 on Figure 4a is smoother and more conformal than Figure 4b,c. These observations are explained by the enhanced nucleation on the S1 sample due to the higher initial concentration of phosphorus oxide. Black circles mark Al_2O_3 clusters in Figure 4b that are ~0.5−1 nm higher than the average surface of the S2 and are randomly distributed. These cluster formations are likely due to the faster nucleation rate on randomly distributed defect regions. The estimated coverage of these clusters is ~4%. In Figure 4c, some pinholes with a depth greater than 1 nm are observed. These pinholes could be indicative of intrinsic or exfoliation-induced defects on black-P.

To compare the Al_2O_3 morphologies of similar thickness between samples with different concentration of phosphorus oxide, 80 cycles of ALD Al_2O_3 is deposited on the S3 sample, where the Al_2O_3 thickness (~2.7 nm) is comparable to that of the S1 sample (~2.47 nm). As seen in Figure 4d, deposition of Al_2O_3 on oxide free black-P results in Al_2O_3 island formation. However, gaps form between neighboring islands, leading to a high surface RMS roughness (0.61 nm) and high depth variation (2 nm on average). This indicates that the surface functionalization or pretreatments[29,33] are still need to improve the Al_2O_3 nucleation and uniform film growth on phosphorus oxide free black-P, similar to that observed on MoS_2 and graphite surfaces with reduced reactivity.[32,34,35] It is also noted that such "pretreatments" resulting in ALD nucleation and growth may actually be associated with residual surface contamination from device fabrication materials (such as solvents or polymers) in prior reports.[32]

The role of other extrinsic impurities is also important to consider, given the relative immaturity of the materials synthesis. Figures S6 and S7 of the Supporting Information show that tin (Sn) and iodine (I) impurities are detected on the S1−S3 samples. As these samples were vapor transport synthesized with Sn and tin(IV) iodide (SnI_4),[36,37] it is possible for Sn and I to condense onto the black-P crystal during the growth cool down procedure. Here the reaction products exist as a compound of SnI_xO_y, with an estimated maximum Sn/P ratio of 0.07 (Figure S7 of the Supporting Information) on the native surface. After the exfoliation, the Sn/P ratio is lower than 0.02 (Figure S7 of the Supporting Information). This suggests that some SnI_xO_y is present in the black-P bulk. However, as discussed in the Supporting Information, the SnI_xO_y does not play a role in the black-P oxidation. In addition, no peak could be identified in the range of 128.2−129.5 eV[38] in the P 2*p* spectra, which rules out substantial Sn−P bonding, within the limits of detection. Nevertheless, the impact of such impurities on the device performance produced from black-P remains to be systematically studied.

4. CONCLUSION

In summary, the impact of phosphorus oxides on the nucleation of atomic layer deposited Al_2O_3 on black-P surfaces has been investigated by *in situ* XPS characterization. A black-P sample that is initially free of detectable phosphorus oxide is robust against oxidation by 200 °C exposures to an ALD environment and exposure to ALD precursors. In contrast, phosphorus oxides, if present on the black-P surface, can change the black-P surface reactivity and can react with the surface physisorbed, adventitious contamination or the H_2O precursor at 200 °C. As a result, the surface oxidation of black-P increases after annealing as well as after the ALD process. It is found that several cycles are required for Al_2O_3 to nucleate on black-P surface, following a "substrate inhibiting growth". SnI_xO_y compounds, byproducts from the black-P growth, are detected on the as received and exfoliated samples as contaminants. Moreover, it appears that phosphorus oxide and possibly surface adventitious contamination on black-P surfaces are possible nucleation sites for ALD of Al_2O_3, which enhance the coverage and the conformality of Al_2O_3 on black-P. When the black-P surface is phosphorus oxide free, a large coverage of Al_2O_3 clusters accompanied by high height depth variation (~2 nm) can be obtained after 80 ALD cycles. It is clear that the starting surface plays a critical role in ALD nucleation and the controlled functionalization methods will need to be developed before the integration of black-P in industrial device processes can be realized.

■ ASSOCIATED CONTENT

Supporting Information

XPS spectra of C 1*s* and O 1*s* core levels; thicknesses calculation of Al_2O_3 and phosphorus oxide; the $I_{P\text{-}O}/I_{P\text{-}P}$ ratio as a function of ALD cycles; effect of the plasmon loss feature of

DOI: 10.1021/acsami.5b03192
ACS Appl. Mater. Interfaces XXXX, XXX, XXX−XXX

Al 2*s* on P 2*p* peak fitting; XPS spectra of Sn 3*d* and I 3*d* core level. The Supporting Information is available free of charge on the ACS Publications website at DOI: 10.1021/acsami.5b03192.

AUTHOR INFORMATION

Corresponding Author

*R. M. Wallace. E-mail: rmwallace@utdallas.edu .

Author Contributions

The paper was written through contributions of all authors. All authors have given approval to the final version of the paper.

Notes

The authors declare no competing financial interest.

ACKNOWLEDGMENTS

This work was supported in part by the SWAN Center, a SRC center sponsored by the Nanoelectronics Research Initiative and NIST, the Center for Low Energy Systems Technology (LEAST), one of the six SRC STARnet Centers, sponsored by MARCO and DARPA, and the US/Ireland R&D Partnership (UNITE) under the NSF award ECCS-1407765.

REFERENCES

(1) Li, L.; Yu, Y.; Ye, G. J.; Ge, Q.; Ou, X.; Wu, H.; Feng, D.; Chen, X. H.; Zhang, Y. Black Phosphorus Field-Effect Transistors. *Nat. Nanotechnol.* **2014**, *9*, 372−377.

(2) Liu, H.; Neal, A. T.; Zhu, Z.; Luo, Z.; Xu, X.; Tománek, D.; Ye, P. D. Phosphorene: An Unexplored 2D Semiconductor with a High Hole Mobility. *ACS Nano* **2014**, *8*, 4033−4041.

(3) Luo, X.; Rahbarihagh, Y.; Hwang, J. C. M.; Liu, H.; Du, Y.; Ye, P. D. Temporal and Thermal Stability of Al_2O_3-Passivated Phosporene MOSFETs. *IEEE Electron Device Lett.* **2014**, *35*, 1−3.

(4) Xia, F.; Wang, H.; Jia, Y. Rediscovering Black Phosphorus as an Anisotropic Layered Material for Optoelectronics and Electronics. *Nat. Commun.* **2014**, *5*, 4458.

(5) Late, D. J. Temperature Dependent Phonon Shifts in Few-Layer Black Phosphorus. *ACS Appl. Mater. Interfaces* **2015**, *7*, 5857−5862.

(6) Late, D. J.; Liu, B.; Matte, H. S. S. R.; Dravid, V. P.; Rao, C. N. R. Hysteresis in Single-Layer MoS_2 Field. *ACS Nano* **2012**, *6*, 5635−5641.

(7) Late, D. J.; Huang, Y. K.; Liu, B.; Acharya, J.; Shirodkar, S. N.; Luo, J.; Yan, A.; Charles, D.; Waghmare, U. V.; Dravid, V. P.; Rao, C. N. R. Sensing Behavior of Atomically Thin-Layered MoS_2 Transistors. *ACS Nano* **2013**, *7*, 4879−4891.

(8) Harada, Y.; Murano, K.; Shirotani, I.; Takahashi, T.; Maruyama, Y. Electronic Structure of Black Phosphorus Studied by X-ray Photoelectron Spectroscopy. *Solid State Commun.* **1982**, *44*, 877−879.

(9) Favron, A.; Gaufrès, E.; Fossard, F.; Lévesque, P. L.; Anne-Laurence; Phaneuf-L' Heureux; Tang, N. Y-W.; Loiseau, A.; Leonelli, R.; Francoeur, S.; Martel, R. Exfoliating Pristine Black Phosphorus Down to the Monolayer: Photo-Oxidation and Quantum Confinement, 2014; arXiv:1408.0345.

(10) Deng, Y.; Lou, Z.; Conrad, N. J.; Han, L.; Gong, Y.; Najmaei, S.; Ajayan, P. M.; Lou, J.; Xu, X.; Ye, P. D. Black Phosphorus-Monolayer MoS_2 van der Waals Heterojunction p-n Diode. *ACS Nano* **2014**, *8*, 8292−8299.

(11) Morita, A. Semiconducting Black Phosphorus. *Appl. Phys. A: Solids Surf.* **1986**, *39*, 227−242.

(12) Kim, J.-S.; Liu, Y.; Zhu, W.; Kim, S.; Wu, D.; Tao, L.; Dodabalapur, A.; Lai, K.; Akinwande, D. Toward Air-Stable Multilayer Phosphorene Thin-Films and Transistors. *Sci. Rep.* **2015**, *5*, 8989.

(13) Wood, J. D.; Wells, S. A.; Jariwala, D.; Chen, K.; Cho, E.; Sangwan, V. K.; Liu, X.; Lauhon, L. J.; Marks, T. J.; Hersam, M. C. Effective Passivation of Exfoliated Black Phosphorus Transistors Against Ambient Degradation. *Nano Lett.* **2014**, *14*, 6964−6970.

(14) Castellanos-Gomez, A.; Vicarelli, L.; Prada, E.; Island, J. O.; Narasimha-Acharya, K. L.; Blanter, S. I.; Groenendijk, D. J.; Buscema, M.; Steele, G. A.; Alvarez, J. V.; Zandbergen, H. W.; Palacios, J. J.; van der Zant, H. S. J. Isolation and Characterization of Few-Layer Black Phosphorus. *2D Mater.* **2014**, *1*, 025001.

(15) Chen, X.; Wu, Y.; Wu, Z.; Xu, S.; Wang, L.; Han, Y.; Han, T.; He, Y.; Cai, Y.; Wang, N. High Quality Sandwiched Black Phosphorus Heterostructure and its Quantum Oscillations. 2014; arXiv:1412.1357v1, pp 1−19.

(16) Gillgren, N.; Wickramaratne, D.; Shi, Y.; Espiritu, T.; Yang, J.; Hu, J.; Wei, J.; Liu, X.; Mao, Z.; Watanabe, K.; Taniguchi, T.; Bockrath, M.; Barlas, Y.; Lake, R. K.; Ning Lau, C. Gate Tunable Quantum Oscillations in Air-Stable and High Mobility Few-Layer Phosphorene Heterostructures. *2D Mater.* **2014**, *2*, 011001.

(17) Li, L.; Ye, G. J.; Tran, V.; Fei, R.; Chen, G.; Wang, H.; Wang, J.; Watanabe, K.; Taniguchi, T.; Yang, L.; Chen, X. H. Quantum Oscillations in Black Phosphorus Two-Dimensional Electron Gas. 2014; arXiv:1411.6572.

(18) Liu, H.; Neal, A. T.; Si, M.; Du, Y.; Ye, P. D. The Effect of Dielectric Capping on Few-Layer Phosphorene Transistors: Tuning the Schottky Barrier Heights. *IEEE Electron Device Lett.* **2014**, *35*, 795−797.

(19) Haratipour, N.; Robbins, M. C.; Koester, S. J. Black Phosphorus p-MOSFETs with High Transconductance and Nearly Ideal Subthreshold Slope. 2014; arXiv:1409.8395, pp 2−4.

(20) Wallace, R. M. In-Situ Studies of Interfacial Bonding of High-k Dielectrics for CMOS Beyond 22nm. *ECS Trans.* **2008**, *16*, 255−271.

(21) Milojevic, M.; Aguirre-Tostado, F. S.; Hinkle, C. L.; Kim, H. C.; Vogel, E. M.; Kim, J.; Wallace, R. M. Half-Cycle Atomic Layer Deposition Reaction Studies of Al_2O_3 on $In_{0.2}Ga_{0.8}As$ (100) Surfaces. *Appl. Phys. Lett.* **2008**, *93*, 202902.

(22) Herrera-Gómez, A.; Hegedus, A.; Meissner, P. L. Chemical Depth Profile of Ultrathin Nitrided SiO_2 Films. *Appl. Phys. Lett.* **2002**, *81*, 1014−1016.

(23) Rokugawa, H.; Adachi, S. Investigation of Rapid Thermally Annealed GaP(001) Surfaces in Vacuum. *Surf. Interface Anal.* **2010**, *42*, 88−94.

(24) Peng, X.; Wei, Q. Chemical Scissors Cut Phosphorene Nanostructures and Their Novel Electronic Properties. 2014; arXiv:1405.0801, pp 1−15.

(25) Brennan, B.; Dong, H.; Zhernokletov, D.; Kim, J.; Wallace, R. M. Surface and Interfacial Reaction Study of Half Cycle Atomic Layer Deposited Al_2O_3 on Chemically Treated InP Surfaces. *Appl. Phys. Express* **2011**, *4*, 125701.

(26) Dong, H.; Brennan, B.; Qin, X.; Zhernokletov, D. M.; Hinkle, C. L.; Kim, J.; Wallace, R. M. In Situ Study of Atomic Layer Deposition Al_2O_3 on GaP (100). *Appl. Phys. Lett.* **2013**, *103*, 121604.

(27) Brennan, B.; Qin, X.; Dong, H.; Kim, J.; Wallace, R. M. In Situ Atomic Layer Deposition Half Cycle Study of Al_2O_3 Growth on AlGaN. *Appl. Phys. Lett.* **2012**, *101*, 211604.

(28) Qin, X.; Brennan, B.; Dong, H.; Kim, J.; Hinkle, C. L.; Wallace, R. M. In Situ Atomic Layer Deposition Study of HfO_2 Growth on NH_4OH and Atomic Hydrogen Treated $Al_{0.25}Ga_{0.75}N$. *J. Appl. Phys.* **2013**, *113*, 244102.

(29) Qin, X.; Dong, H.; Brennan, B.; Azacatl, A.; Kim, J.; Wallace, R. M. Impact of N_2 and Forming Gas Plasma Exposure on the Growth and Interfacial Characteristics of Al_2O_3 on AlGaN. *Appl. Phys. Lett.* **2013**, *103*, 221604.

(30) Ziletti, A.; Carvalho, A.; Trevisanutto, P. E.; Campbell, D. K.; Coker, D. F.; Castro Neto, A. H. Phosphorene Oxides: Bandgap Engineering of Phosphorene by Oxidation. *Phys. Rev. B* **2015**, *91*, 85407.

(31) Puurunen, R. L. Surface Chemistry of Atomic Layer Deposition: A Case Study for the Trimethylaluminum/Water Process. *J. Appl. Phys.* **2005**, *97*, 121301.

(32) McDonnell, S.; Brennan, B.; Azcatl, A.; Lu, N.; Dong, H.; Buie, C.; Kim, J.; Hinkle, C. L.; Kim, M. J.; Wallace, R. M. HfO_2 on MoS_2 by Atomic Layer Deposition: Adsorption Mechanisms and Thickness Scalability. *ACS Nano* **2013**, *7*, 10354−10361.

DOI: 10.1021/acsami.5b03192
ACS Appl. Mater. Interfaces XXXX, XXX, XXX−XXX

(33) Cheng, L.; Qin, X.; Lucero, A. T.; Azcatl, A.; Huang, J.; Wallace, R. M.; Cho, K.; Kim, J. Atomic Layer Deposition of a High-k Dielectric on MoS_2 Using Trimethylaluminum and Ozone. *ACS Appl. Mater. Interfaces* **2014**, *6*, 11834−11838.
(34) Pirkle, A.; Wallace, R. M.; Colombo, L. In Situ Studies of Al_2O_3 and HfO_2 Dielectrics on Graphite. *Appl. Phys. Lett.* **2009**, *95*, 133106.
(35) Pirkle, A.; McDonnell, S.; Lee, B.; Kim, J.; Colombo, L.; Wallace, R. M. The Effect of Graphite Surface Condition on the Composition of Al_2O_3 by Atomic Layer Deposition. *Appl. Phys. Lett.* **2010**, *97*, 82901.
(36) Lange, S.; Schmidt, P.; Nilges, T. Au_3SnP_7@Black Phosphorus: An Easy Access to Black Phosphorus. *Inorg. Chem.* **2007**, *46*, 4028−4035.
(37) Köpf, M.; Eckstein, N.; Pfister, D.; Grotz, C.; Krüger, I.; Greiwe, M.; Hansen, T.; Kohlmann, H.; Nilges, T. Access and in Situ Growth of Phosphorene-Precursor Black Phosphorus. *J. Cryst. Growth* **2014**, *405*, 6−10.
(38) Xian, A.-P.; Gong, G.-L. Surface Oxidation of Molten Sn-0.07 Wt% P in Air at 280 °C. *J. Mater. Res.* **2008**, *23*, 1532−1536.

DOI: 10.1021/acsami.5b03192
ACS Appl. Mater. Interfaces XXXX, XXX, XXX−XXX